Molecular Characterization of Rheumatoid Arthritis with Magnetic Resonance Imaging

Jeffrey T. Gu, B.S.[1], **Linda Nguyen, B.S.**[1], **Abhijit J. Chaudhari, Ph.D.**[2], and **John D. MacKenzie, M.D.**[1]

[1]Radiology and Biomedical Imaging, UCSF, San Francisco, CA

[2]Department of Radiology, University of California Davis School of Medicine, Sacramento, CA

Abstract

Several recent advances in the field of magnetic resonance imaging (MRI) may transform the detection and monitoring of rheumatoid arthritis (RA). These advances depict both anatomic and molecular alterations from RA. Previous techniques could detect specific end products of metabolism *in vitro*, or were limited to providing anatomic information. This review focuses on the novel molecular imaging techniques of hyperpolarized carbon-13 (^{13}C) MRI, MRI with iron labeled probes, and fusion of MRI with positron emission tomography. These new imaging approaches go beyond the anatomic description of RA and lend new information into the status of this disease by giving molecular information.

INTRODUCTION

Relatively new magnetic resonance imaging (MRI) techniques have the potential to transform the workup and management of patients with rheumatoid arthritis (RA). These MRI techniques detect or localize molecular imaging probes. This work opens up new directions for the evolution of MRI as this imaging technique moves beyond anatomic to molecular characterization of disease processes.

The detection of disease severity and treatment monitoring in RA would benefit from more sophisticated non-invasive strategies. Current clinical imaging relies on the depiction of anatomic changes from RA in and around the joints using conventional radiography, ultrasound, computed tomography, and MRI.[1–3] However, these imaging strategies tend to show later stages of disease, which may translate into a delay in treatment.

Current clinical strategies for detecting disease also have limitations. Clinical measures of improvement are often subjective—sometimes relying on clinical opinion alone—and can take months to years for changes to be detectable in the patient.[4] Although the clinical response to the treatment is often measured by comparing the average improvement for each of the outcomes measured, such methods may fall short when considering conditions where all patients improved modestly, or where half of patients improved markedly with the other half improving little at all.[5]

Corresponding Author: John D. MacKenzie, MD University of California San Francisco Department of Radiology and Biomedical Imaging 505 Parnassus Avenue San Francisco, CA 94143-0628 Office: 415 514-6330 john.mackenzie@ucsf.edu.

Several clinical trials have shown the efficacy of early and aggressive treatment,[6,7] and imaging approaches that identify patients for early intervention could potentially reduce functional deterioration and improve long-term outcome.[8,9] In addition, efficacy of therapy has been inconsistent, and have relied mainly on detecting the endpoints of autoimmune pathological processes to treat disease.[10] Disease relapse is common and medications are often expensive and associated with marked toxicities.

There is great potential for more accurate diagnosis and improved monitoring during treatment. One strategy that has received much attention and effort has been to detect serum biomarkers.[11] Other metabolic imaging methods are available, but until recently, none have demonstrated widespread clinical use.[3]

HYPERPOLARIZED ^{13}C MRI

Hyperpolarized carbon-13 (^{13}C) MRI represents a new and still relatively uncharted area for molecular characterization of disease processes. Preliminary data suggest that this technique may be promising for RA.[12,13] While conventional MRI primarily depicts anatomic structures with exquisite resolution and tissue contrast, hyperpolarized ^{13}C MRI detects and localizes carbon based imaging probes. These ^{13}C imaging probes are typically injected into the bloodstream. MRI detects the localization and metabolism of the probe. The imaging of the ^{13}C probe can also be fused with anatomic/conventional (proton=^{1}H) MRI for further disease characterization.

Prior to refinement of the hyperpolarization method, magnetic resonance spectroscopic imaging (MRSI) of ^{13}C compounds had been plagued by low sensitivity due to the low polarization of nuclei at thermal equilibrium. With ^{1}H imaging, the low sensitivity is compensated by the abundance of ^{1}H in biological tissues. Without the use of hyperpolarization ^{13}C imaging is restricted by both the low gyromagnetic ratio and low in vivo abundance of ^{13}C.[14,15] Hyperpolarization techniques have now been developed in the solid state to increase polarization by five orders of magnitude,[16] allowing for spectroscopic measurements using a ^{13}C probe to achieve spectral resolution of the chemical shifts of the probe along with its metabolic products. The fusion of conventional anatomic and novel molecular imaging presents a new non-invasive imaging strategy to probe normal biologic and disease processes.

Hyperpolarization by Dynamic Nuclear Polarization

Nuclear magnetic resonance (NMR) utilizes the interaction of atomic nuclei that have a non-zero nuclear spin with an external magnetic field. In the past, increases in magnetic field have been used to enhance polarization. However, higher fields present problems with limited depths of radiofrequency penetration and alterations in tissue contrast. Dynamic nuclear polarization (DNP) solves this through transferring the high polarization of electron spins to coupled nuclear spins by subjecting samples to a high magnetic field at cryogenic temperatures.[16] The frozen sample is then rapidly dissolved to create a hyperpolarized liquid with a signal that decays with the molecular T_1 constant as the nuclei return to their equilibrium polarization.

The hyperpolarized nuclei are typically introduced intravenously to the subject and the nuclei elaborate radiofrequency (RF) signal that is detected by the MRI scanner. This allows for direct visualization, and quantification of the probe and its metabolites, where signal is directly proportional to the concentration of the agent.[14] This imaging scheme is possible on clinical 3 Tesla systems after implementation of hardware and software modifications, including dedicated or dual ^{1}H/^{13}C coils, broadband capability, and dedicated pulse sequences for ^{13}C spectral imaging. Additionally, due to the low natural abundance of ^{13}C

in the human body, hyperpolarized ^{13}C images enjoy the benefit of minimal background signal, with a signal to noise ratio (SNR) of greater than 10,000 times that of non-polarized samples.[16,17]

Limitations of Hyperpolarized Imaging Agents

The utilization of hyperpolarized imaging agents comes with a few restrictions. Current techniques rely on hyperpolarization of the probe outside the subject since the ideal conditions for preparation require low temperature and microwave irradiation.[17] Furthermore, the longitudinal relaxation rate T_1 of the imaging agent must also be sufficiently long in biological fluids to allow for the substance to be distributed to the target organ before the hyperpolarization effects have vanished, restricting the time window for clinical diagnostic imaging to two to three times the T_1. As with many emerging technologies, the technique relies on sophisticated technology with limited availability requiring expensive resources and expert personnel.

APPLICATIONS OF HYPERPOLARIZED ^{13}C MRI FOR RA

^{13}C Pyruvate as a Molecular Probe

To date the most extensively examined ^{13}C imaging probe has been ^{13}C-pyruvate and initial data suggest that hyperpolarized MRI with ^{13}C-pyruvate may be applicable for arthritis detection (Figure 1). Pyruvate has many properties that make it an ideal candidate as a non-invasive imaging biomarker of inflammatory arthritis. Pyruvate is an endogenous molecule with a low toxicity profile and can be rapidly hyperpolarized with a relatively long T_1 relaxion of ~60 seconds in solution and 30–40 seconds in vivo.

Pyruvate occupies a key intersection in several metabolic pathways as an intermediary in energy metabolism in living cells. Because inflamed tissues have increased energy demands, differentiation between normal and diseased tissues is possible. Levels of pyruvate are elevated in joints affected by osteoarthritis[18] and the amount of lactic acid, a metabolic product of pyruvate, is elevated in the synovial fluid of patients with rheumatoid arthritis.[19] Inhibitors of pyruvate metabolism downregulate inflammation.[20] Proton (^{1}H) NMR studies have also demonstrated elevated lactate in the synovial fluid and synovium of patients with rheumatoid arthritis and in rodent models of inflammatory arthritis.[21–24]

The technique of hyperpolarized ^{13}C MRI relies on obtaining spectroscopic information of the imaging probe (pyruvate) and its subsequent conversion into metabolites such as lactate (Figure 2). The molecular information can be readily combined with anatomic data on conventional MRI (Figure 1). This fusion imaging pinpoints disease location and may provide a quantifiable measurement of traditionally qualitative values of disease severity.[12]

The ability of hyperpolarized ^{13}C MRI to measure a treatment response has yet to be tested. If this technique finds clinical utility, the imaging findings using ^{13}C-pyruvate will likely need to be placed in context of the treatment regimen. Steroids used to treat RA also alter pyruvate/glucose metabolism, thus the subgroup of patients on steroid treatment will likely have a unique metabolism profile depicted on MRI.

Clinical potential for hyperpolarized MRI with ^{13}C-pyruvate is already showing promise. This technique is attractive for human translation because hyperpolarized ^{13}C-pyruvate has FDA IND approval and a phase I clinical trial using this imaging strategy in prostate cancer patients has just been successfully completed. Given this groundwork, if pilot studies for RA in animal models continue to be successful, this potential clinical application should progress quickly for patients with RA.

Additional Molecular Probes

Several additional ^{13}C probes have been tested in disease models and several may be helpful in RA. These probes are largely biomolecules with altered metabolism in disease states.[25] Although these compounds are conceivable for application to RA, they are currently not as far along in development as ^{13}C-pyruvate, and further investigation remains necessary to promote their use.

The hyperpolarization technique also allows for the simultaneous injection of multiple ^{13}C compounds. Multi-metabolite polarization has been explored to circumvent the long polarization times of DNP. Polarization of multiple metabolites may give a greater scope of measureable parameters, such as perfusion using ^{13}C urea, and metabolism using ^{13}C pyruvate.[26] Additionally, polarization of multiple metabolites from separate or related enzymatic pathways during the same imaging session may provide additional disease specific information. This would usher in a new era using a single *in vivo* scan that is either utilized for several diseases or provides more combined specific information of any one particular disease.

IMAGING RA WITH SPIONs

Superparamagnetic iron oxide nanoparticles (SPIONS) are well-tested contrast agents that have been applied primarily in animal models to image a broad range of diseases and conditions such as atherosclerosis, cancer, multiple sclerosis, spinal cord injury, and stroke.[27] Research has also pointed to a potential clinical application for RA.[28–32] SPIONs are biocompatible due to their organic coating and iron in the SPION core can be incorporated into the plasma iron pool where it is used in the normal metabolic pathways of the body and secreted.[33] Importantly, because SPIONs can be targeted to specific cellular processes for imaging, RA may be detected and quantified in its early stages.

MRI detection of SPIONs

SPIONs create contrast on MRI by greatly shortening T_1 relaxation times, thus SPION probes show up as areas of low to absent signal intensity on MR imaging. The basic structure of a SPION is an iron oxide core surrounded by a surface layer. The core is usually comprised of magnetite (Fe_3O_4) or maghemite (γ-Fe_2O_3), where the former's biocompatibility has already been proven.[34] In superparamagnetism, the magnetic domains formed by ferrous (Fe^{2+}) and ferric (Fe^{3+}) ions of the core align to an applied external magnetic field; the resultant magnetic moment and magnetic susceptibilities are greater than those of paramagnetic materials such as gadolinium chelates.[35] With a higher magnetic moment and susceptibility, SPIONs create larger disturbances in the local magnetic field and therefore are more efficient at dephasing the spins of surrounding water protons in the tissue. Thus, SPIONs shorten T1 and T2/T2* relaxation times more than gadolinium-based contrast agents.[33] Like paramagnetic materials, SPIONs lose their magnetization with removal of the external magnetic field.

Tissue Specific Targeting

SPIONs can be designed to target a wide variety of tissues. Encapsulating the core, the hydrophilic surface layer—made of polymers or organic molecules—prevents the aggregation of SPIONs *in vivo*[36] and also facilitates targeting.[37] Nanoparticle size and surface coatings of tissue-specific ligands or specific molecular precursors direct the particle to areas of interest[37] through distinct means: size passively directs SPIONs via naturally guided physiological processes, whereas surface layer modifications actively direct SPIONs via targeting against specific molecules.[38]

Distinguished by their hydrodynamic diameter, the three general classes of SPIONs are oral SPIONs (300 nm-3.5 um), standard SPIONs (50–150 nm), and ultrasmall SPIONs (<50 nm).[39] Oral SPIONs are ingested; because they are too large to be absorbed, distribution occurs throughout the GI tract for imaging of the abdomen.[33] Standard SPIONs are quickly taken up by the hepatic and splenic cells of the mononuclear phagocyte system (MPS) upon intravenous administration, while ultrasmall SPIONs have a longer blood half-life and so are able to accumulate in the lymph nodes and bone marrow.[33]

Active targeting is accomplished through several approaches. In intracellular trapping,[40] conjugation of receptor-specific ligands to the nanoparticle coating allows for directed uptake of SPIONs by the cells of interest.[38] Another related method for targeting utilizes streptavidin-conjugated SPIONs. Biotinylated antibodies are administered intravenously and localize to the desired imaging site. Because streptavidin has an extraordinarily high binding affinity for biotin, the streptavidin-conjugated SPIONs are directed to the desired area.[41] Beyond targeting of SPIONs to specific areas for imaging, SPIONs may facilitate detection of enzymatic activity *in vivo*. In the presence of particular enzymes, SPIONs can self-assemble thereby causing a decrease in spin-spin relaxation time.[31]

Rationale for SPION in Rheumatoid Arthritis

SPIONs are an attractive molecular imaging strategy for use in RA for several reasons. Because SPIONs are phagocytosed by macrophages, sites of inflammation can be pinpointed in RA patients. The amount of signal loss created by SPIONs may correlate with the degree of inflammation in the patient. In one study, the magnitude of T_2 signal reduction was found to correlate with macrophage content in atherosclerotic plaque.[42] This has implications for RA because the abundance of macrophages in the inflamed synovium is indicative of RA severity.[28] Additionally, Beckmann et al. showed that signal loss also correlates to a treatment effect; particularly, with dexamethasone treatment of antigen-induced arthritic rats, signal attenuation was seen in the synovium, which was not detected in placebo-treated arthritic rats.[28]

Several SPIONs have been designed with targeting ligands that localize to sites of inflammation. Examples of these ligands are hyaluronic acid which target activated macrophages;[43] a peptide sequence that binds endothelial vascular adhesion molecule-1 (VCAM-1), a protein on the endothelium upregulated in inflammation[40] and implicated in RA disease processes;[44] and an antibody specific for E-selectin, another adhesion molecule expressed on the endothelium under inflammatory conditions.[32] The lack of ionizing radiation also makes this approach attractive for repeated monitoring.

Presently, gadolinium-based contrast agents are used for RA monitoring and help characterize synovitis.[45] However, this method detects changes on a macroscopic level and presumably at later stages when irreversible arthritic damage has already occurred.[29] Since SPIONs target the cellular and molecular level,[30] it is conceivable that more subtle arthritic changes may be detected and monitored.

Specific SPIONs for RA

SPIONs have been used to image various aspects of inflammation: macrophages in antigen-induced arthritis;[28–30] expression of E-selectin;[32] and myeloperoxidase activity, an enzyme implicated in inflammation.[31] Ferumoxtran (Combidex®, Sinerem®) is an ultrasmall SPION that was used in the first study imaging a murine RA model with SPIONs. It has a mean diameter of approximately 20–30 nm and a coating of dextran. The stabilizing dextran coating confers an increased plasma half-life, which is reported to be 24–36 hours in humans.[27] Because of their coating and ultrasmall size, ferumoxtran has a wide

biodistribution allowing for nanoparticle phagocytosis by monocytes and macrophages outside the MPS.[46] In that first study, nanoparticles were found to accumulate in greater amounts in the arthritic synovium compared to controls with intraarticular injection of SPIONs; hence, more SPIONs were phagocytosed by cells of the arthritic synovium than in the control.[29] This resulted in a marked signal loss in the joint of arthritic mice compared to control mice.

Lutz et al. applied this same SPION in a rabbit model of RA (Figure 3). The authors showed that both perfusion characteristics and macrophage presence in the synovium could be monitored in arthritic joints of rabbits.[30] The above studies lay the foundation for SPIONs utilization in patients to assess RA disease levels through detection and monitoring of the synovium for macrophage activity.

Further specificity for inflammation may be conferred when SPIONs are crosslined to anti-E-selectin monoclonal antibodies or substrates of myeloperoxidase (MPO). The antibody targets SPIONs to sites of inflammation where E-selectin is upregulated: an adhesion molecule on vascular endothelial cells that helps circulating leukocytes migrate into inflamed tissues.[47] SPION labeled anti-E-selectin antibodies localize to sites of inflammation and are visible on MRI.[32] Another approach that uses enzymatic activity to detect inflammation is with SPIONs conjugated to serotonin, a substrate of MPO. In this presence of MPO these SPIONs produce tyrosyl radicals forming o,o-dityrosine crosslinks between nanoparticles thereby self-assembling in solution; aggregations of these particles alter T_2 relaxation times and are visible on MRI.[31]

Challenges for SPION Imaging in RA

Although SPIONs likely have low toxicity,[33] further safety testing in humans will be necessary to understand the potential side-effects. In vitro studies suggest that SPION may cause DNA damage, oxidative stress, and epigenetic effects.[48] Furthermore, SPIONs may present a logistical problem in clinical practice. After intravenous administration, localization of the probe takes at least 24 hours, so pre-and post-injection imaging requires two imaging sessions spaced at least 24 hours apart and co-registration of the pre- and post-contrast enhanced images can be challenging.

COMBINED MRI AND PET

Recent technological advances have merged MRI and positron emission tomography (PET) into a single imaging system. This promising combination of anatomic and molecular imaging is available in the clinic and currently undergoing testing for RA. The near simultaneous acquisition of molecular PET and anatomic MRI information is attractive since disease activity on PET may be correlated with bone and joint changes on high-resolution MRI (Figure 4). One rationale for this approach is that molecular processes precede anatomical changes in RA, therefore PET may better depict and quantify early disease.

^{18}F-fluorodeoxyglucose (^{18}F-FDG) is the most widely used and available molecular probe for PET, and it has already shown utility in identifying sites of inflammation. PET with ^{18}F-FDG reveals leukocyte activity and accumulates at sites of infection[49] and synovitis in RA.[50] The pannus formation of synovitis typically precedes cartilage and bone destruction visible on radiography.[1–3] Leukocytes including macrophages localize at sites of inflammation and have increased energy demands. This localization and increased glucose utilization favors accumulation of ^{18}F-FDG and subsequent depiction on PET.

The power of dual MRI-PET is the ability to create a map of inflammation. Regions of ^{18}F-FDG uptake are co-registered with the underlying changes in morphology on conventional

MRI: pannus formation, bone marrow edema, erosions, and cartilage loss. However, PET can detect picomolar fluctuations in radiotracer concentration[51] and offers a detection sensitivity orders of magnitude higher than MRI.

Several additional molecular probes beyond ^{18}F-FDG are in development, including radiolabeled receptor ligands, peptides, antibodies, and cells.[52] These probes target other important pathological processes that may be of utility in patients with RA, such as hypoxia and angiogenesis.[53,54]

Another important component of the probe that is amenable for modification in PET is the radioisotope label. The 110 minute half-life ($t_{1/2}$) of ^{18}F is practical for clinical applications: the isotope remains around long enough to allow for probe localization and imaging and subsequently decays, thus minimizing exposure to ionizing radiation. Other radioisotopes, such as ^{15}O ($t_{1/2}$=122 seconds), ^{11}C ($t_{1/2}$=20 minutes) or ^{64}Cu ($t_{1/2}$=12.7 hours), further expand the range of options by weighing the benefits of fast scan times and reduced radiation dose versus signal quality and practicality.

Although one benefit of MRI is the higher spatial resolution (< 1 mm) far above that afforded by high-resolution clinical PET systems (~2–3 mm), the primary advantage of MRI is its exquisite tissue contrast: MRI depicts alternations in cartilage, bone, fluid, muscle, tendon, and soft tissue,[1–3] whereas PET and PET/CT are much more limited in tissue contrast. The anatomic changes of RA are also well depicted on conventional MRI.[1–3]

The MRI-PET approach can help overcome a few limitations of conventional MRI in RA patients. First, RA patients have an increased prevalence of renal insufficiency,[55] which would preclude the use of gadolinium due to the potential association with nephrogenic systemic fibrosis.[56] Contrast-agent-free MRI fused with PET may provide a viable option for measuring disease activity in these patients. Sites of inflammation can be studied on a joint-by-joint basis or throughout the body using whole body MRI techniques[57,58] and quantitative measurements may be performed on multiple lesions.[59]

MRI alone presents several challenges in quantitative analysis. Spatial and temporal variations in signal intensity owing to factors such as RF inhomogeneity and gradient non-linearity can compromise MRI contrast quantification.[60,61] This becomes a critical issue especially in a longitudinal setting. Also, dynamic contrast enhanced imaging with MRI is challenging with variations in heart rate, tissue temperature and disease status.[62,63] The addition of PET measurements may help minimize these inherent limitations as well as validate promising quantitative MRI techniques.

Current evidence for use of dual MRI-PET in RA

Several lines of evidence suggest that a dual imaging approach may help with RA disease detection and monitoring. Although the role of PET is well established in the field of oncology, several studies have demonstrated the utility of PET for RA. PET can depict and quantify synovitis,[50,64,65] bone marrow edema,[66] and inflammation.[67,68]

PET systems used in those studies were conventional and designed to image large organs or the whole human body. While they are suitable for scanning joints like the knee, shoulder or the spine in RA patients, their quantification ability is limited when imaging small joints such as those in the hands and feet.[65] Extending the capabilities of PET to small joints will be critical given the propensity of RA to affect the small joints.[69]

Early attempts at a multimodality approach have demonstrated some success in the dual imaging approach for small joints. One system targeted the extremities of RA patients and

was capable of combined high resolution PET and computed tomography.[70,71] Pilot studies have confirmed the feasibility of combining information on high-resolution extremity PET/CT with subsequently co-registered of MRI data.[72] The PET and MR images were fused using immobilizing equipment and co-registration software based on the intermediate CT providing anatomical correlation.[73] The spatial resolution of the PET component for this system was ~2.5 mm as opposed to the 5–6 mm afforded by conventional systems. This system provides a combined 3D map of the anatomic and molecular status of the disease with metabolic activity depicted by PET and adjacent erosions and bone marrow edema depicted by MRI (Figure 4).

PET systems have recently been introduced to operate inside conventional MRI systems as `inserts' and perform truly simultaneous MRI-PET imaging.[51,74,75] A recent report by Miese et al.[76] used the newly available MR-compatible BrainPET insert (Siemens Healthcare, Erlangen, Germany) to perform simultaneous imaging of the hand in an RA patient. The MRI field strength used was 3.0T and the PET spatial resolution was ~3 mm. Several other manufacturers are beginning to introduce whole-body MRI-PET systems, but to date, fusion imaging with clinical systems has yet to be reported in a cohort of patients with RA. For this to be accomplished however MRI-PET systems must produce quantitatively accurate images, a problem that currently remains challenging.[77,78]

Dual MRI-PET Applications for RA

The complementary molecular and anatomic information provided by dual MRI-PET may benefit early therapeutic monitoring for RA. The availability of this powerful non-invasive imaging tool coincides with several new treatment options.[79] Since predicting remission is important but currently limited to score-based methods[80] and timing of treatment affects prognosis,[81] dual MRI-PET may benefit RA patients by providing a rapid and detailed assessment of disease status and treatment response.

Initial clinical evidence suggests that ^{18}F-FDG-PET imaging of the wrist and hand may help predict early response (in < 5 weeks) to treatment before clinical score changes.[71,82] The clinical scoring based on a physical examination is typically performed at three months after initiation of treatment. PET therefore may stratify responders from non-responders at early time-points compared to other imaging techniques or physical examination and hence potentially improve treatment outcome.

MRI has established scoring systems for the manifestations of RA,[83] in addition to providing anatomic localization of radiotracer activity (Figure 4). Metrics derived from MRI-PET have potential to become surrogate markers for rapid evaluation of existing and new drugs.[72,76] But this and the test characteristics for dual MRI-PET compared to either MRI or PET alone need further study.

The quantitative aspects of MRI-PET make it suitable for staging RA and hence determining the optimal therapeutic regimen. Assessment of multiple joints in the extremity can provide a unique snapshot of disease severity. The whole-body MRI-PET systems can interrogate the entire body and produce a total score similar to a physician exam.[57] The benefits of extremity and whole-body scanning may be complementary, but the advantages must be traded off with data acquisition time and cost of these systems. Scanners acquiring PET and MRI data simultaneously will have an advantage in this area, but are likely to be more expensive than their separate PET/CT or MRI counterparts.

The most interesting application from a basic science standpoint is that of improving our current understanding of the pathology at the target tissue in RA *in vivo* and the pathogenesis of the disease. High-resolution PET systems will be useful in this regard since

they offer improved visualization and quantification of molecular events.[72,84] The ultimate goal may be to implement high-resolution imaging on both PET and MRI over the whole body.

Challenges for Dual MRI-PET

Major considerations associated with the clinical implementation of MRI-PET imaging are the use of radioactive probes and high cost. Improved detection systems and strategies have enhanced image quality in the past decade with equal amounts of radiation doses and relatively short scan times. Imaging protocols that reduce overall radiation burden and discomfort to the patient must be designed. This is particularly important when repeatedly scanning using MRI-PET. Methods to correlate identical sites of inflammation over time on longitudinal studies will be important. Increased spatial resolution over the whole body as described above is also an unmet goal. Despite these limitations, dual MRI-PET presents unique opportunities and the possibility of improved diagnosis and treatment monitoring for RA patients.

CONCLUSION

This is an exciting time for the field of MRI with several emerging molecular imaging strategies in development for application in RA. MRI with hyperpolarized carbon-13 compounds may yield new insight into disease metabolism and treatment monitoring. Both iron-based particles and dual MRI-PET may help better define areas of inflammation and signal disease severity and treatment response. All three of these non-invasive imaging strategies have strengths as well as weaknesses and more work is needed before they prove useful in patients with RA. The promise is earlier detection and better monitoring of disease and response to treatment.

References

1. MacKenzie, JD.; Karasick, D. Imaging of Rheumatoid Arthritis. In: Weissman, B., editor. Imaging of Arthritis and Metabolic Bone Disease. Elsevier Health Sciences; Philadelphia: 2009. p. 340-64.

2. Sommer OJ, Kladosek A, Weiler V, Czembirek H, Boeck M, Stiskal M. Rheumatoid Arthritis: A Practical Guide to State-of-the-Art Imaging, Image Interpretation, and Clinical Implications1. Radiographics. 2005; 25:381–98. [PubMed: 15798057]

3. McQueen FM, Ostergaard M. Established rheumatoid arthritis - new imaging modalities. Best Pract Res Clin Rheumatol. 2007; 21:841–56. [PubMed: 17870031]

4. Scott DL, Kingsley GH. Tumor necrosis factor inhibitors for rheumatoid arthritis. N Engl J Med. 2006; 355:704–12. [PubMed: 16914706]

5. Felson DT, Anderson JJ, Boers M, et al. American College of Rheumatology. Preliminary definition of improvement in rheumatoid arthritis. Arthritis Rheum. 1995; 38:727–35. [PubMed: 7779114]

6. Emery P. Evidence supporting the benefit of early intervention in rheumatoid arthritis. J Rheumatol Suppl. 2002; 66:3–8. [PubMed: 12435162]

7. Guidelines for the management of rheumatoid arthritis: 2002 Update. Arthritis Rheum. 2002; 46:328–46. [PubMed: 11840435]

8. Conaghan PG, Bird P, McQueen F, et al. The OMERACT MRI inflammatory arthritis group: advances and future research priorities. J Rheumatol. 2009; 36:1803–5. [PubMed: 19671816]

9. McQueen FM, Dalbeth N. Predicting joint damage in rheumatoid arthritis using MRI scanning. Arthritis Res Ther. 2009; 11:124. [PubMed: 19796371]

10. Gompels LL, Paleolog EM. A window on disease pathogenesis and potential therapeutic strategies: molecular imaging for arthritis. Arthritis Res Ther. 2011; 13:201. [PubMed: 21345267]

11. Taylor P, Gartemann J, Hsieh J, Creeden J. A systematic review of serum biomarkers anti-cyclic citrullinated Peptide and rheumatoid factor as tests for rheumatoid arthritis. Autoimmune Dis. 2011; 2011:815038. [PubMed: 21915375]

12. MacKenzie JD, Yen YF, Mayer D, Tropp JS, Hurd RE, Spielman DM. Detection of inflammatory arthritis by using hyperpolarized 13C-pyruvate with MR imaging and spectroscopy. Radiology. 2011; 259:414–20. [PubMed: 21406626]

13. Larson PE, Gold GE. Science to practice: Can inflammatory arthritis be monitored by using MR imaging with injected hyperpolarized 13C-pyruvate? Radiology. 2011; 259:309–10. [PubMed: 21502386]

14. Mansson S, Johansson E, Magnusson P, et al. 13C imaging-a new diagnostic platform. Eur Radiol. 2006; 16:57–67. [PubMed: 16402256]

15. Kohler SJ, Yen Y, Wolber J, et al. In vivo 13 carbon metabolic imaging at 3T with hyperpolarized 13C-1-pyruvate. Magn Reson Med. 2007; 58:65–9. [PubMed: 17659629]

16. Ardenkjaer-Larsen JH, Fridlund B, Gram A, et al. Increase in signal-to-noise ratio of > 10,000 times in liquid-state NMR. Proc Natl Acad Sci U S A. 2003; 100:10158–63. [PubMed: 12930897]

17. Golman K, Ardenkjaer-Larsen JH, Petersson JS, Mansson S, Leunbach I. Molecular imaging with endogenous substances. Proc Natl Acad Sci U S A. 2003; 100:10435–9. [PubMed: 12930896]

18. Damyanovich AZ, Staples JR, Chan AD, Marshall KW. Comparative study of normal and osteoarthritic canine synovial fluid using 500 MHz 1H magnetic resonance spectroscopy. J Orthop Res. 1999; 17:223–31. [PubMed: 10221839]

19. Falchuk KH, Goetzl EJ, Kulka JP. Respiratory gases of synovial fluids. An approach to synovial tissue circulatory-metabolic imbalance in rheumatoid arthritis. Am J Med. 1970; 49:223–31. [PubMed: 5452943]

20. Fink MP. Ethyl pyruvate: a novel anti-inflammatory agent. J Intern Med. 2007; 261:349–62. [PubMed: 17391109]

21. Hitchon CA, El-Gabalawy HS, Bezabeh T. Characterization of synovial tissue from arthritis patients: a proton magnetic resonance spectroscopic investigation. Rheumatol Int. 2009; 29:1205–11. [PubMed: 19184029]

22. Meshitsuka S, Yamazaki E, Inoue M, Hagino H, Teshima R, Yamamoto K. Nuclear magnetic resonance studies of synovial fluids from patients with rheumatoid arthritis and osteoarthritis. Clin Chim Acta. 1999; 281:163–7. [PubMed: 10217637]

23. Naughton D, Whelan M, Smith EC, Williams R, Blake DR, Grootveld M. An investigation of the abnormal metabolic status of synovial fluid from patients with rheumatoid arthritis by high field proton nuclear magnetic resonance spectroscopy. FEBS Lett. 1993; 317:135–8. [PubMed: 8381364]

24. Naughton DP, Haywood R, Blake DR, Edmonds S, Hawkes GE, Grootveld M. A comparative evaluation of the metabolic profiles of normal and inflammatory knee-joint synovial fluids by high resolution proton NMR spectroscopy. FEBS Lett. 1993; 332:221–5. [PubMed: 7691662]

25. Gallagher FA, Bohndiek SE, Kettunen MI, Lewis DY, Soloviev D, Brindle KM. Hyperpolarized 13C MRI and PET: in vivo tumor biochemistry. J Nucl Med. 2011; 52:1333–6. [PubMed: 21849405]

26. Wilson DM, Keshari KR, Larson PE, et al. Multi-compound polarization by DNP allows simultaneous assessment of multiple enzymatic activities in vivo. J Magn Reson. 2010; 205:141–7. [PubMed: 20478721]

27. Corot C, Petry KG, Trivedi R, et al. Macrophage imaging in central nervous system and in carotid atherosclerotic plaque using ultrasmall superparamagnetic iron oxide in magnetic resonance imaging. Invest Radiol. 2004; 39:619–25. [PubMed: 15377941]

28. Beckmann N, Falk R, Zurbrügg S, Dawson J, Engelhardt P. Macrophage infiltration into the rat knee detected by MRI in a model of antigen-induced arthritis. Magnetic Resonance in Medicine. 2003; 49:1047–55. [PubMed: 12768583]

29. Dardzinski BJ, Schmithorst VJ, Holland SK, et al. MR imaging of murine arthritis using ultrasmall superparamagnetic iron oxide particles. Magn Reson Imaging. 2001; 19:1209–16. [PubMed: 11755731]

30. Lutz AM, Seemayer C, Corot C, et al. Detection of synovial macrophages in an experimental rabbit model of antigen-induced arthritis: ultrasmall superparamagnetic iron oxide-enhanced MR imaging. Radiology. 2004; 233:149–57. [PubMed: 15333767]

31. Perez JM, Simeone FJ, Tsourkas A, Josephson L, Weissleder R. Peroxidase substrate nanosensors for MR imaging. Nano Lett. 2004; 4:119–22.

32. Reynolds PR, Larkman DJ, Haskard DO, et al. Detection of vascular expression of E-selectin in vivo with MR imaging. Radiology. 2006; 241:469–76. [PubMed: 17005768]

33. Wang YX, Hussain SM, Krestin GP. Superparamagnetic iron oxide contrast agents: physicochemical characteristics and applications in MR imaging. Eur Radiol. 2001; 11:2319–31. [PubMed: 11702180]

34. Gupta AK, Gupta M. Synthesis and surface engineering of iron oxide nanoparticles for biomedical applications. Biomaterials. 2005; 26:3995–4021. [PubMed: 15626447]

35. Kooi, ME.; Heeneman, S.; Daemen, MJAP.; Engelshoven, JMAv; Cleutjens, KBJM. The Emerging Role of USPIOs for MR Imaging of Atherosclerosis. In: Bulte, JWM.; Modo, MMJ., editors. Nanoparticles in Biomedical Imaging. Springer; New York: 2008. p. 63-90.

36. Peng XH, Qian X, Mao H, et al. Targeted magnetic iron oxide nanoparticles for tumor imaging and therapy. Int J Nanomedicine. 2008; 3:311–21. [PubMed: 18990940]

37. Lodhia J, Mandarano G, Ferris N, Eu P, Cowell S. Development and use of iron oxide nanoparticles (Part 1): Synthesis of iron oxide nanoparticles for MRI. Biomed Imaging Interv J. 2010; 6:e12. [PubMed: 21611034]

38. Thorek DL, Chen AK, Czupryna J, Tsourkas A. Superparamagnetic iron oxide nanoparticle probes for molecular imaging. Ann Biomed Eng. 2006; 34:23–38. [PubMed: 16496086]

39. Elias A, Tsourkas A. Imaging circulating cells and lymphoid tissues with iron oxide nanoparticles. ASH Education Program Book. 2009; 2009:720–6.

40. Kelly KA, Allport JR, Tsourkas A, Shinde-Patil VR, Josephson L, Weissleder R. Detection of vascular adhesion molecule-1 expression using a novel multimodal nanoparticle. Circ Res. 2005; 96:327–36. [PubMed: 15653572]

41. Artemov D, Mori N, Okollie B, Bhujwalla ZM. MR molecular imaging of the Her-2/neu receptor in breast cancer cells using targeted iron oxide nanoparticles. Magn Reson Med. 2003; 49:403–8. [PubMed: 12594741]

42. Morishige K, Kacher DF, Libby P, et al. High-resolution magnetic resonance imaging enhanced with superparamagnetic nanoparticles measures macrophage burden in atherosclerosis. Circulation. 2010; 122:1707–15. [PubMed: 20937980]

43. Kamat M, El-Boubbou K, Zhu DC, et al. Hyaluronic acid immobilized magnetic nanoparticles for active targeting and imaging of macrophages. Bioconjug Chem. 2010; 21:2128–35. [PubMed: 20977242]

44. Wellicome SM, Kapahi P, Mason JC, Lebranchu Y, Yarwood H, Haskard DO. Detection of a circulating form of vascular cell adhesion molecule-1: raised levels in rheumatoid arthritis and systemic lupus erythematosus. Clin Exp Immunol. 1993; 92:412–8. [PubMed: 7685670]

45. Mundinger A, Ioannidou M, Meske S, Dinkel E, Beck A, Sigmund G. MRI of knee arthritis in rheumatoid arthritis and spondylarthropathies. Rheumatol Int. 1991; 11:183–6. [PubMed: 1784887]

46. Di Marco M, Sadun C, Port M, Guilbert I, Couvreur P, Dubernet C. Physicochemical characterization of ultrasmall superparamagnetic iron oxide particles (USPIO) for biomedical application as MRI contrast agents. Int J Nanomedicine. 2007; 2:609–22. [PubMed: 18203428]

47. Kansas GS. Selectins and their ligands: current concepts and controversies. Blood. 1996; 88:3259–87. [PubMed: 8896391]

48. Singh, N.; Jenkins, GJS.; Asadi, R.; Doak, SH. Potential toxicity of superparamagnetic iron oxide nanoparticles (SPION). 2010.

49. Dumarey N, Egrise D, Blocklet D, et al. Imaging Infection with 18F-FDG-Labeled Leukocyte PET/CT: Initial Experience in 21 Patients. J Nucl Med. 2006; 47:625–32. [PubMed: 16595496]

50. Roivainen A, Parkkola R, Yli-Kerttula T, et al. Use of positron emission tomography with methyl-11C-choline and 2-18F-fluoro-2-deoxy-glucose in comparison with magnetic resonance imaging for the assessment of inflammatory proliferation of synovium. Arthritis & Rheumatism. 2003; 48:3077–84. [PubMed: 14613269]

51. Cherry SR, Louie AY, Jacobs RE. The integration of positron emission tomography with magnetic resonance imaging. Proceedings of the IEEE. 2008; 96:416–38.

52. Phelps ME. PET: The Merging of Biology and Imaging into Molecular Imaging. Journal of Nuclear Medicine. 2000; 41:661. [PubMed: 10768568]

53. Kim JH, Lee JS, Kang KW, et al. Whole-Body Distribution and Radiation Dosimetry of (68)Ga-NOTA-RGD, a Positron Emission Tomography Agent for Angiogenesis Imaging. Cancer Biother Radiopharm. 2011

54. Gaertner FC, Souvatzoglou M, Brix G, Beer AJ. Imaging of hypoxia using PET and MRI. Curr Pharm Biotechnol. 2012

55. Karstila K, Korpela M, Sihvonen S, Mustonen J. Prognosis of clinical renal disease and incidence of new renal findings in patients with rheumatoid arthritis: follow-up of a population-based study. Clinical Rheumatology. 2007; 26:2089–95. [PubMed: 17492249]

56. Deo A, Fogel M, Cowper SE. Nephrogenic systemic fibrosis: a population study examining the relationship of disease development to gadolinium exposure. Clinical Journal of the American Society of Nephrology. 2007; 2:264–7. [PubMed: 17699423]

57. Kubota K, Ito K, Morooka M, et al. FDG PET for rheumatoid arthritis: basic considerations and whole-body PET/CT. Ann N Y Acad Sci. 2011; 1228:29–38. [PubMed: 21718320]

58. Kubota K, Ito K, Morooka M, et al. Whole-body FDG-PET/CT on rheumatoid arthritis of large joints. Ann Nucl Med. 2009; 23:783–91. [PubMed: 19834653]

59. Fox JJ, Autran-Blanc E, Morris MJ, et al. Practical approach for comparative analysis of multilesion molecular imaging using a semiautomated program for PET/CT. J Nucl Med. 2011; 52:1727–32. [PubMed: 21984797]

60. Schenck J. The role of magnetic susceptibility in magnetic resonance imaging: MRI magnetic compatibility of the first and second kinds. Medical Physics. 1996; 23:815. [PubMed: 8798169]

61. Bernstein M, Huston J 3rd, Ward H. Imaging artifacts at 3.0 T. Journal of magnetic resonance imaging: JMRI. 2006; 24:735. [PubMed: 16958057]

62. Boesen M, Østergaard M, Cimmino MA, Kubassova O, Jensen KE, Bliddal H. MRI quantification of rheumatoid arthritis: current knowledge and future perspectives. European Journal of Radiology. 2009; 71:189–96. [PubMed: 19477615]

63. Kubassova O, Boesen M, Cimmino MA, Bliddal H. A computer-aided detection system for rheumatoid arthritis MRI data interpretation and quantification of synovial activity. European Journal of Radiology. 2010; 74:e67–e72. [PubMed: 19411154]

64. Palmer WE, Rosenthal DI, Schoenberg OI, et al. Quantification of inflammation in the wrist with gadolinium-enhanced MR imaging and PET with 2-[F-18]-fluoro-2-deoxy-D-glucose. Radiology. 1995; 196:647–55. [PubMed: 7644624]

65. Beckers C, Ribbens C, Andre B, et al. Assessment of Disease Activity in Rheumatoid Arthritis with 18F-FDG PET. J Nucl Med. 2004; 45:956–64. [PubMed: 15181130]

66. Nakamura H, Masuko K, Yudoh K, et al. Positron emission tomography with 18F-FDG in osteoarthritic knee. Osteoarthritis and Cartilage. 2007; 15:673–81. [PubMed: 17336549]

67. Hustinx R, Malaise MG. PET Imaging of Arthritis. PET Clinics. 2006; 1:131–9.

68. Goerres GW, Forster A, Uebelhart D, et al. F-18 FDG whole-body PET for the assessment of disease activity in patients with rheumatoid arthritis. Clin Nucl Med. 2006; 31:386–90. [PubMed: 16785804]

69. Fleming A, Crown J, Corbett M. Early rheumatoid disease. I. Onset. Annals of the Rheumatic Diseases. 1976; 35:357.

70. Bowen SL, Wu Y, Chaudhari AJ, et al. Initial characterization of a dedicated breast PET/CT scanner during human imaging. Journal of Nuclear Medicine. 2009; 50:1401–8. [PubMed: 19690029]

71. Chaudhari AJ, Bowen SL, Burkett GW, et al. High-resolution 18F-FDG PET with MRI for monitoring response to treatment in rheumatoid arthritis. European Journal of Nuclear Medicine and Molecular Imaging. 2010; 37:1047. [PubMed: 20119695]

72. Chaudhari AJ, Ferrero A, Godinez F, et al. Molecular Imaging of Rheumatoid, Psoriatic and Osteoarthritis in the Hand [abstract]. Arthritis Rheum. 2011; 63(Suppl 10):206.

73. Chaudhari, AJ.; Burkett, GW.; Bowen, SL., et al. Multimodality high resolution wrist imaging for monitoring response to therapy in rheumatoid arthritis: Instrumentation and techniques. IEEE Nuclear Science Symposium Conference Record; IEEE; 2008. p. 4840-4.2008

74. Catana C, Procissi D, Wu Y, et al. Simultaneous in vivo positron emission tomography and magnetic resonance imaging. Proceedings of the National Academy of Sciences. 2008; 105:3705.

75. Judenhofer MS, Wehrl HF, Newport DF, et al. Simultaneous PET-MRI: a new approach for functional and morphological imaging. Nature medicine. 2008; 14:459–65.

76. Miese F, Scherer A, Ostendorf B, et al. Hybrid 18 F-FDG PET-MRI of the hand in rheumatoid arthritis: initial results. Clinical Rheumatology. 2011; 30:1247–50. [PubMed: 21590292]

77. Herzog H, Pietrzyk U, Shah NJ, Ziemons K. The current state, challenges and perspectives of MR-PET. NeuroImage. 2010; 49:2072–82. [PubMed: 19853045]

78. Catana C, van der Kouwe A, Benner T, et al. Toward implementing an MRI-based PET attenuation-correction method for neurologic studies on the MR-PET brain prototype. Journal of Nuclear Medicine. 2010; 51:1431–8. [PubMed: 20810759]

79. Horton SC, Emery P. Biological therapy for rheumatoid arthritis: where are we now? Br J Hosp Med (Lond). 2012; 73:12–8. [PubMed: 22241404]

80. Ma MH, Ibrahim F, Walker D, et al. Remission in Early Rheumatoid Arthritis: Predicting Treatment Response. J Rheumatol. 2012

81. Lard LR, Visser H, Speyer I, et al. Early versus delayed treatment in patients with recent-onset rheumatoid arthritis: comparison of two cohorts who received different treatment strategies. The American journal of medicine. 2001; 111:446–51. [PubMed: 11690569]

82. Elzinga EH, van der Laken CJ, Comans EFI, et al. 18F-FDG PET as a tool to predict the clinical outcome of infliximab treatment of rheumatoid arthritis: an explorative study. Journal of Nuclear Medicine. 2011; 52:77. [PubMed: 21149486]

83. Ostergaard M, Peterfy C, Conaghan P, et al. OMERACT Rheumatoid Arthritis Magnetic Resonance Imaging Studies. Core set of MRI acquisitions, joint pathology definitions, and the OMERACT RA-MRI scoring system. J Rheumatol. 2003; 30:1385–6. [PubMed: 12784422]

84. Tan AL, Tanner S, Waller M, et al. Regional Differences in Bone Metabolism in the DIP Joint in Psoriatic Arthritis Compared to Osteoarthritis Support the Concept of An Integrated Bone-Enthesis Nail Apparatus - A High-Resolution 18F-Fluoride Positron Emission Tomography Study [abstract]. Arthritis Rheum. 2011; 63(Suppl 10):1702.
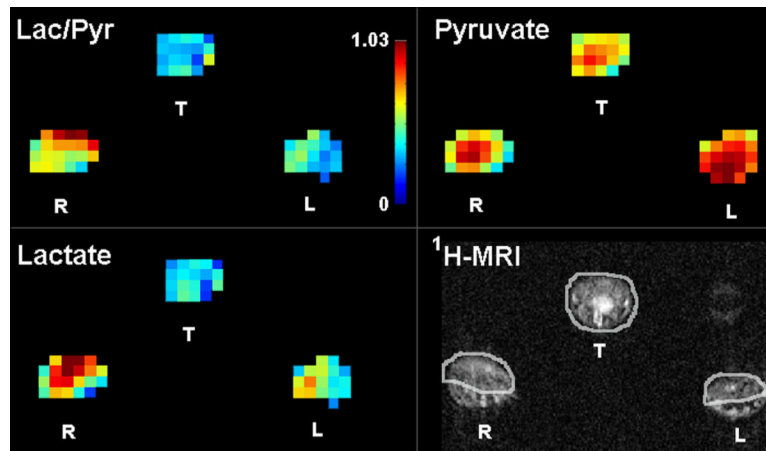
Figure 1.
Quantitative metabolic maps in an arthritic rat after injection of hyperpolarized ^{13}C-pyruvate show increased lactate production in the arthritic right paw as measured by the lactate-to-pyruvate ratio (Lac/Pyr). The color bar indicates relative levels of Lac/Pyr. Red color is the maximum signal intensity for ^{13}C-pyruvate = 1485 au, ^{13}C-lactate = 674 au, and Lac/Pyr = 1.03. ^{1}H-MRI shows soft tissue swelling in the arthritic right (R) paw in comparison to the control left (L) paw and the region of interest analysis applied for the metabolic maps. T=tail, au=arbitrary units. Reproduced with permission from MacKenzie JD, et al. Radiology 2011.[12]
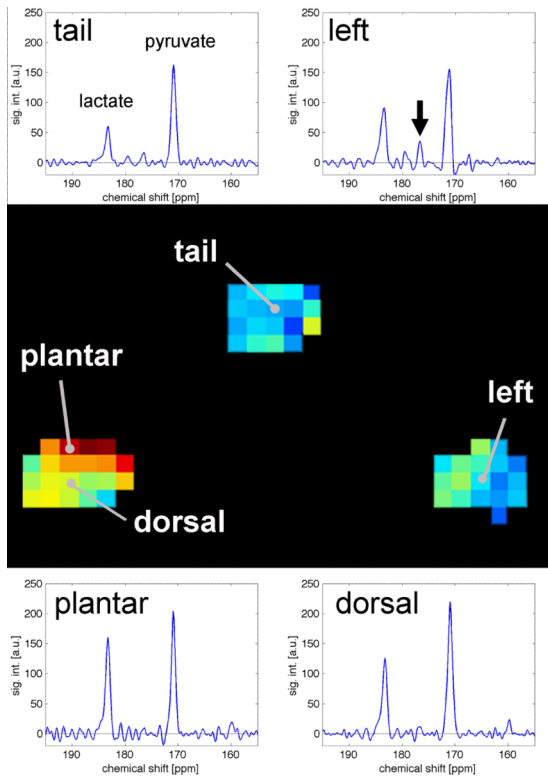
Figure 2.
Spectroscopic profiles from single 2.5 × 2.5 × 10 mm voxels in control and arthritic tissues in one rat. Increased ^{13}C-lactate production is demonstrated in the plantar surface of the arthritic right paw (lactate-to-pyruvate ratio = 0.70) in comparison to the control left paw (= 0.57), tail (= 0.37), and tissues away from the site of arthritis induction in the dorsal right paw (= 0.57). Arrow indicates alanine production in the control left paw, but no alanine is observed in the arthritic paw. Reproduced with permission from MacKenzie JD, et al. Radiology 2011.[12]
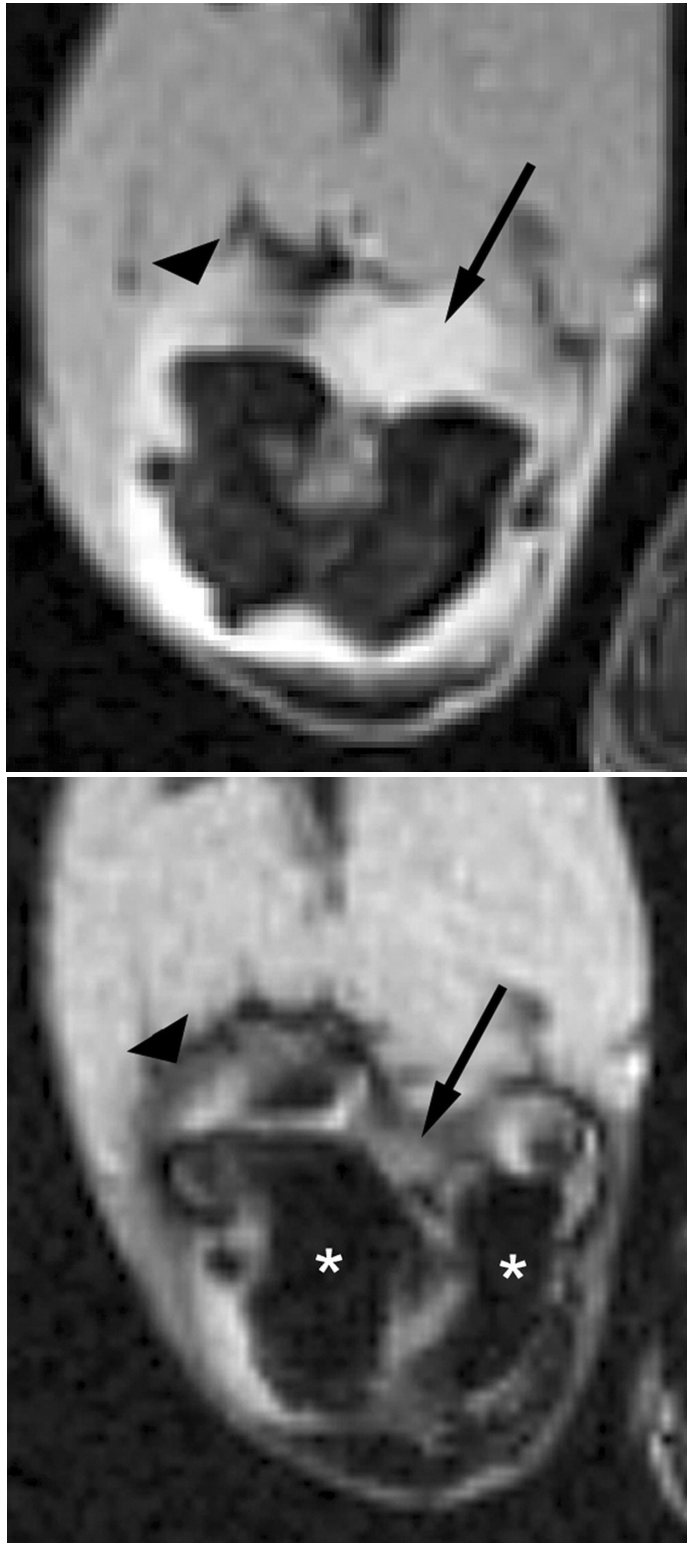
Figure 3.
Transverse T2*-weighted fast gradient-echo images (1000/15; flip angle, 25°) show T2* effects at USPIO-enhanced MR imaging of macrophage activity in antigen-induced arthritis

in rabbits. (a) Precontrast image shows joint effusion (arrow) that is surrounded by a thickened synovium (arrowhead). (b) Postcontrast image (24 hours after USPIO administration) shows susceptibility effects (arrow) within the synovium (arrowhead), representing USPIO uptake in phagocytic-active macrophages. Signal intensity of bone marrow (*) is decreased in comparison to that in a, which is caused by USPIO uptake by the mononuclear phagocyte system within the bone marrow. Reproduced with permission from Lutz AM, et al. Radiology 2004.[30]
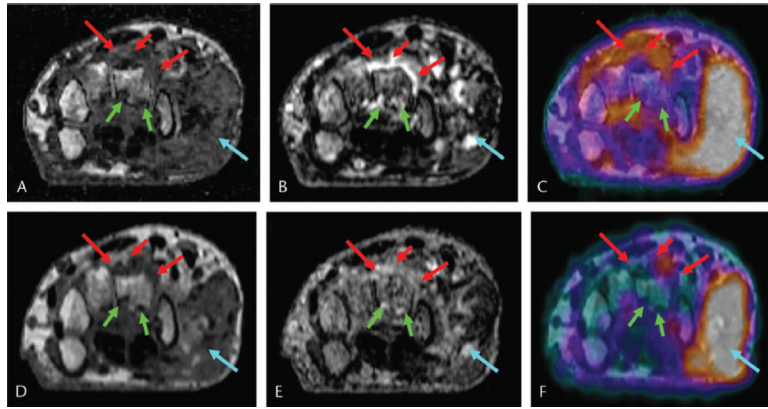
Figure 4.
Fusion of high-resolution ^{18}F-FDG-PET with MRI for an RA therapy responder. Images were generated using the clinical MRI and high resolution PET/CT sequential scanning approach.[71] The top row shows images from baseline while the bottom row depicts images at 4 weeks after the initiation of treatment. Figures (a) and (c) depict representative axial sections from a pre-contrast T_1-weighted MR image of the patient's wrist, (b) and (d) show the same section from the T_1-weighted MR image acquired post-administration of a gadolinium-based contrast agent, and (c) and (f) demonstrate the MRI-PET fusion images of the same section. Red arrows show synovitis in the carpal region, green arrows indicate inflammation at sites of erosions while the blue arrows indicate inflammation at the base of the thumb (corresponding to osteoarthritis). Dramatic reductions in synovitis and metabolic activity at sites of erosions were measured from MRI-PET at 4 weeks and correlated with the rheumatologist's score obtained at the patient's 3-month standard-of-care visit.